Available online at www.sciencedirect.com

ScienceDirect

Proceedings of the Combustion Institute 39 (2023) 735–743

Proceedings of the Combustion Institute

www.elsevier.com/locate/proci

Gas-Phase Reaction

Shock tube/laser absorption measurement of the rate constant of the reaction: $H_2O_2 + CO_2$ 2OH + CO_2

Jiankun Shao, Rishav Choudhary, David F. Davidson*, Ronald K. Hanson

Department of Mechanical Engineering, Stanford University, 418 Panama Street, Bldg 660 Room 104, Stanford, CA 94305, United States

Received 23 November 2021; accepted 3 August 2022
Available online 1 October 2022

Abstract

We address the role of the linear mixing rule in the kinetics of the H_2O_2 decomposition system by reporting the rate constant for $H_2O_2 + M = 2OH + M$ (M = Ar and CO_2) in the temperature range of 1087–1234 K at low pressures in a mixture of 20% CO_2 in Argon. The reaction rate constant was inferred from H_2O concentrations monitored by using a laser-absorption spectroscopy-based water diagnostic. To the best of our knowledge, this is the first measurement of the rate constant of this reaction in a mixture to be reported in literature. A significant discrepancy was found between the rate constants derived using the traditional linear mixing rule and the reduced pressure linear mixing rule. This discrepancy can have serious implications on the predictive accuracy of these kinetic models, especially under conditions relevant to the operation of supercritical CO_2 (sCO_2) power cycles that rely on oxy-fuel combustion in a working fluid comprised almost entirely of CO_2.
© 2022 The Combustion Institute. Published by Elsevier Inc. All rights reserved.

Keywords: Hydrogen peroxide decomposition; Supercritical carbon dioxide; Reaction rate constant; Linear mixing rule

1. Introduction

The U.S. Energy Information Administration (EIA), in its Annual Energy Outlook 2021 (AEO2021), has projected that the U.S. electricity generation will increase by 35% from 2020 to 2050 [1]. To mitigate the accompanying increase in the cost of power generation, it is imperative to power future power generation plants by advanced power cycles that offer greater thermal efficiency and lower emissions [2]. One of the focuses of these studies is the development of direct fired sCO_2 cycles, which are expected to rely on oxy-fuel combustion as the source of enthalpy. The combustors that are needed for these cycles need to operate under conditions of heavy CO_2 dilution. However, the effects of high carbon dioxide dilution on combustion kinetics and dynamics are not well understood.

Our understanding of the kinetic effects of CO_2 addition is almost exclusively based on studies where the carbon mole fraction in the mixture is less than 10% [3]. Very few kinetic studies have been conducted at the expected operating conditions of direct-fired sCO_2 power cycles ($Xco_2 > 96\%$). Shao et al. published an ignition delay time dataset for hydrogen and methane at high CO_2 dilution (up to 86%) conditions [4]. Their

* Corresponding author.
E-mail address: dfd@stanford.edu (D.F. Davidson).

https://doi.org/10.1016/j.proci.2022.08.021
1540-7489 © 2022 The Combustion Institute. Published by Elsevier Inc. All rights reserved.

study provides the first experimental evidence that two well-known combustion kinetic mechanisms [5,6] diverge at these elevated test conditions, even though they are consistent at low CO_2 concentration conditions. Their observations were further corroborated by Karimi et al. [7], who measured the IDT of methane at pressures of 100 and 200 atm, between 1139 and 1410 K diluted in 86% CO_2. Burke et al. [8] studied the dependence of mass burning rates in $H_2/CO/O_2$ flames on CO_2 dilution. They report a stronger pressure and temperature dependence of mass burning rates with increasing CO_2 dilution. Global combustion properties like IDTs, mass burning rates, and flame speeds, reported in such datasets are invaluable to modelers who use them to validate, improve, and develop more accurate kinetic models. However, the sensitivity of these quantities themselves is dominated by a handful of key elementary reactions. The accuracy of the predictive capability of these kinetic models, therefore, depends on the accuracy of these key elementary reaction rate constants [9,10]. Unfortunately, the impact of high CO_2 dilution on the rate constants of some of these reactions is not well known [11].

Masunov et al. [12] and Wait et al. [13] have studied the impact of carbon dioxide dilution on the rate constant of some bimolecular elementary reactions theoretically, by solving the master kinetic equation. They report that CO_2 dilution has a catalytic effect on some of these reactions under certain conditions of temperature and pressure. However, this effect is less pronounced at temperatures representative of sCO_2 combustors. As reported in [4], the sensitivity of IDTs of syngas/oxygen mixtures in an sCO_2 environment is dominated by reactions involving H_2O_2 and HO_2. Two pressure-dependent reactions that dominate the sensitivity are

$$H_2O_2(+M) = OH + OH(+M) \quad \text{(R1)}$$

$$H + O_2(+M) = HO_2(+M) \quad \text{(R2)}$$

Under the conditions relevant to sCO_2 combustors, the rate constant of these reactions will depend strongly on the amount of CO_2. CO_2 acts as a more effective collision partner for exchanging energy with the vibrationally excited dissociation/recombination products than N_2 and Ar, the diluents commonly used in multiple previous experimental investigations of the rate constants of R1 and R2. Recent experimental studies of R2 [14,15] suggest that the chaperon efficiencies of CO_2 used in kinetic models are incorrect and need revision.

While R2 has been extensively studied experimentally and theoretically, studies of R1 reported in literature are sparse. The thermal decomposition of hydrogen peroxide, R1, is the dominant chain-branching reaction for hydrocarbons in the intermediate temperature regime (850–1200 K) [16,17]. Troe et al. conducted the pioneering studies on this reaction rate constant using a shock tube and UV absorption spectroscopy at 215 and 290 nm [18–20]. Those early studies were affected by inherent difficulties, such as measurement sensitivity and interfering species. Modern studies have leveraged advanced diagnostics to provide the measurements with narrower uncertainties. Hong et al. [21,22] studied this reaction using laser absorption of water near 2.5 μm and Sajid et al. [23] studied this reaction using laser absorption of hydrogen peroxide near 7.7 μm. Those studies provided consistent low-pressure-limit rate constants within tight uncertainty bounds with argon and nitrogen as collision partners. Most of the recent kinetic models use the rate constants suggested by Troe [24] in his review that was based on the conclusions drawn from ab initio calculations, theoretical modeling and limited experimental data. These kinetic models provide the reaction rate constant with carbon dioxide as a ratio against the reaction rate constant with argon or nitrogen. The ratio of the third body collision efficiencies of carbon dioxide and argon suggested by Troe [24] is about 1.6, which is largely based on an experimental study conducted at low temperatures (478–896 K) and was published in 1959 [25]. The current study provides the first measurement of this reaction rate constant with carbon dioxide as the collision partner at high temperatures (>1087 K) and in a mixture with a major collision partner, Argon. The measurements and their analysis provide evidence of the inadequacy of the linear mixing rule when used to predict the effective reaction rate constants in mixtures such as these. The reaction rate constant was determined by measuring water forming upon thermal decomposition of H_2O_2 using a laser absorption diagnostic. This study emphasizes the need for improved measurements of the collision efficiency of CO_2 for reactions relevant to oxy-fuel combustion in an sCO_2 combustor.

2. Experimental methods

2.1. Shock tubes

The low-pressure-limit reaction rate constant measurements of hydrogen peroxide decomposition were conducted on the Flexible Applications Shock Tube (FAST) facility at Stanford. FAST has an internal diameter of 14.0 cm, a 2.53 m long driver and a 9.45 m long driven section. Helium was used as the driver gas for all shock experiments. Typical test times at the test conditions explored in this work are 1–2 milliseconds on FAST. The test times can be further extended with well-designed driver inserts when needed. The observation ports in the test sections are located at 1 cm away from the endwall on FAST. The experiments utilized polycarbonate diaphragms. Further details about

Stanford shock tube facilities can be found in Cassady et al. [26] and Shao et al. [27].

The shock arrival times in the driven section of the shock tube were recorded by five piezoelectric pressure transducers located at known distances from the end wall. The velocity of the incident shock at the end wall was then determined by extrapolation, allowing calculation of the initial reflected shock temperature and pressure, using one-dimensional shock-jump relations and assuming vibrational equilibrium and frozen chemistry, with resulting uncertainties in initial post-shock temperature and pressure of less than ±1%.

2.2. Hydrogen peroxide precursor

High-temperature chemical kinetics studies of mixtures with hydrogen peroxide are complicated by the high reactivity of hydrogen peroxide and the lack of an easy-to-use hydrogen peroxide precursor. Most previous researchers have used high-concentration hydrogen peroxide solutions (99%) as the source of hydrogen peroxide [20]. A less volatile and less corrosive precursor would be preferred. In this study, we used a commercially available H_2O_2-urea adduct as the precursor for H_2O_2 (provided by Sigma Aldrich). The adduct is a solid, which makes it easy to handle. Successful use of this material as a gas-phase hydrogen peroxide precursor was demonstrated by Ludwig et al. [28] and Hong et al. [21]. Approximately 25 g of hydrogen peroxide-urea tablets were pulverized and mixed with roughly an equal amount of sand (SiO_2, Sigma-Aldrich) in a flask to prevent agglomeration. The flask was sealed with a rubber stopper and placed in a water bath maintained at 45 °C monitored by a thermocouple. The gradual heating resulted in the release of H_2O_2 in gas phase. Research grade argon and/or carbon dioxide (99.999%) were circulated through the flask for about 15 min. This procedure leads to a seeding of 800–2000 ppm H_2O_2 in the bath gas. This mixture was then directed into the driven section of the shock tube using a filling port 5 cm away from the endwall test section to reduce hydrogen peroxide decomposition on the steel surface of the shock tube. Some of the seeded H_2O_2 decomposed during the filling procedure and after the incident shock. The pre-shock H_2O_2 concentration was determined by taking the difference between the initial and final H_2O concentrations. It was assumed that H_2O and O_2 are the only products of decomposition in this analysis. As described later, the H_2O concentration was monitored by a laser-absorption spectroscopy-based water diagnostic. The pre-shock H_2O_2 decomposition products, i.e., H_2O, and O_2, also act as collision partners during shock-induced decomposition of H_2O_2, however, as described later, the uncertainty in the R1 rate constant stemming from them was quantified to be less than 1% in our experiments.

2.3. Water diagnostic

Laser absorption spectroscopy was used to measure the water time histories. The mole fractions of the absorbing species were inferred by measuring the transmitted (I_t) signal recorded upon the passage of the reflected shock against the vacuum recorded incident (I_0) signal using the Beer-Lambert relation (Eq. (1)), expressed here for a specific wavelength.

$$\alpha_\nu = -\ln\left(\frac{I_t}{I_0}\right)_\nu = k_\nu L \tag{1}$$

where, L is the path length of absorption, and k_ν is spectral absorption coefficient, which can be expressed as Eq. (2).

$$k_\nu = S(T)\Phi_\nu P x_i \tag{2}$$

where, $S(T)$ is the line strength, Φ_ν is the line shape function, P is pressure, and x_i is the mole fraction of the absorber. In the current study, the water concentration time histories were measured using tunable diode laser absorption of water at 2482 nm (4029.52 cm^{-1}). This line was selected because of its large line strength and it has been well characterized by Goldenstein et al. [29]. Infrared radiation was generated using a distributed feedback (DFB) diode laser centered near 2.48 μm from Nanoplus™. A combination of temperature and injection current was carefully adjusted using commercial controllers to achieve the targeted laser wavelength and intensity. A bandpass filter was used to block the broad band emission signals, and a negligible amount of emission was detected during a shock with blocked laser beam. A 1 MHz bandwidth InSb detector was used to monitor the laser intensity in these experiments. The detector was cooled using liquid nitrogen for 40 min before experiments. The absorption cross-section of water at the line-center was measured in a separate set of experiments to further verify the diagnostic.

3. Results and discussion

3.1. Rate constant measurement of $H_2O_2+Ar\rightarrow 2OH+Ar$

A total of seven experiments were conducted using argon as the bath gas. Six additional experiments were conducted with mixtures containing CO_2. The details of the latter are provided in the following section. In order to minimize the uncertainty associated with the rate constant of R1, the test conditions were optimized to suppress the sensitivity of water time histories to secondary reactions. To achieve this, sensitivity analyzes were conducted using the NUI-Syngas mechanism [30]. The sensitivity coefficient, α, is the partial derivative of a species mole fraction with respect to the rate constant parameter A of a reaction, which is a built-in

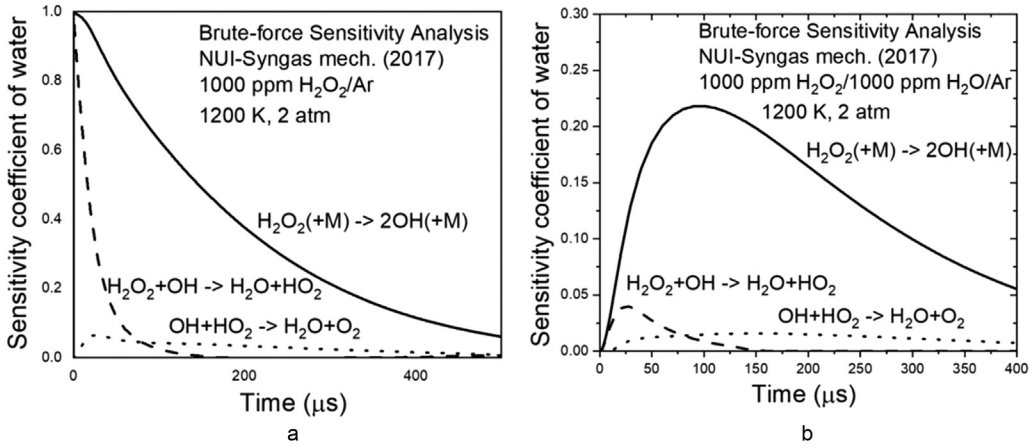

Fig. 1. Brute-force sensitivity analysis of water formation for a) 1000 ppm H_2O_2/Ar mixture at 1200 K and 2 atm; b) 1000 ppm H_2O_2/1000 ppm H_2O/Ar mixture at 1200 K and 2 atm (Only the three largest sensitivities are shown).

function in Chemkin Pro™ software package and can be expressed as Eq. (3).

$$\alpha_{ij}(t) = \left(dx_j/x_j\right)/(dA_i/A_i) \tag{3}$$

Here, x_j is the mole fraction of species j and A_i is the temperature-independent factor of the rate constant of reaction i. Fig. 1 show the brute-force sensitivity analysis of water for 1000 ppm H_2O_2/Ar and 1000 ppm H_2O_2/1000 ppm H_2O/Ar mixtures at 1200 K and 2 atm. The difference between the two mixtures is that the later contains 1000 ppm of water, which is representative of the concentration of water present in partially decomposed hydrogen peroxide/argon mixtures. As stated earlier, a fraction of H_2O_2 decomposes during the filling procedure of the mixture into the shock tube. The decomposition products are primarily water and oxygen. It is this mixture that eventually gets shock-heated. For each experiment, the actual concentration of water in the mixture prior to getting shocked was inferred using the water diagnostic. The sensitivity analysis suggests that water formation in both mixtures is predominantly controlled by R1. Among the secondary reactions contributing to the sensitivity, R3 and R4 are most important. However, the absolute sensitivity of both these reactions is diminished in the second mixture. This suggests that the actual mixture containing partially decomposed H_2O_2 is better suited for determining the rate constant of R1 as the contribution of secondary reactions to the overall uncertainty is expected to be lower. Similar sensitivity analyzes for mixtures with carbon dioxide can be found in the Supplementary Material.

$$H_2O_2 + OH = H_2O + HO_2 \tag{R3}$$

$$OH + HO_2 = H_2O + O_2 \tag{R4}$$

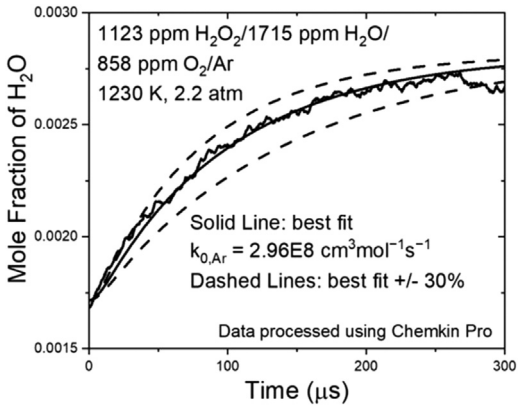

Fig. 2. Measured water time history and the best-fit rate constant ($k_{0,Ar} = 2.96 \times 10^8$ $cm^3mol^{-1}s^{-1}$, using Chemkin Pro) with a mixture of 1123 ppm H_2O_2/1715 ppm H_2O/Ar at 1230 K, 2.2 atm.

Sensitivity analyzes performed using other kinetic models [5,6] led to similar results.

Time histories of water absorbance were recorded and converted into mole fractions using Beer's law at the aforementioned test conditions. The current measurements were conducted in the pressure range of 2.21–2.43 atm. Previous studies [21,23] have suggested that there is negligible difference in the rate constants measured between 1 and 2 atm. Moreover, at these pressures, the rate constant is expected to be close to its low-pressure limit. Therefore, in this study, we have only adjusted the low-pressure limit of the rate constant to match our measurements. Fig. 2 shows a representative water mole fraction profile recorded at 1230 K and 2.2 atm with a mixture of 1123 ppm H_2O_2/1715 ppm H_2O/858 ppm O_2/Ar. Other

Table 1
Reaction rate constant measurement of $H_2O_2 + Ar \rightarrow 2OH + Ar$.

T (K)	P (atm)	$[H_2O]$ (ppm)	$[H_2O_2]$ (ppm)	$k_{0,Ar}$ ($cm^3mol^{-1}s^{-1}$)
1230	2.2	1715	1123	2.96×10^8
1166	2.3	773	1004	1.44×10^8
1135	2.4	453	530	8.16×10^7
1226	2.2	539	794	2.80×10^8
1171	2.3	1936	1011	1.22×10^8
1228	2.2	927	839	2.88×10^8
1175	2.3	531	675	1.39×10^8

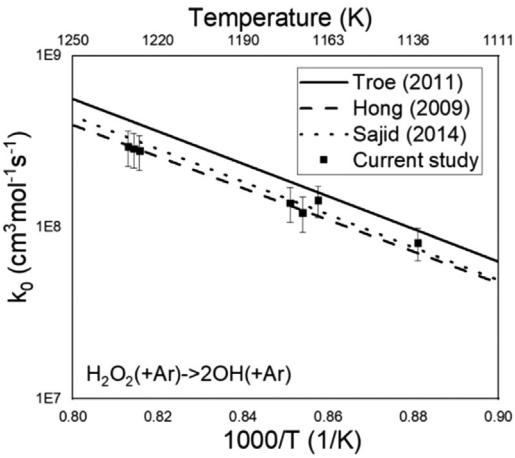

Fig. 3. Arrhenius plot for H_2O_2+Ar→2OH+Ar in low-pressure-limit.

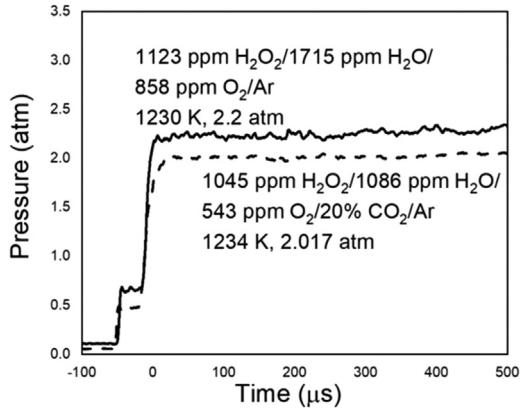

Fig. 4. Pressure trace comparison between a mixture diluted in pure argon and a mixture diluted in 20% CO_2/argon. Solid line: 1230 K; dashed line: 1234 K.

experiments for mixtures diluted in argon can be found in Supplementary Material. The dissociation rate constant with argon as the collision partner, R1 (M = Ar), is reported as the second order rate constant of reaction with units of $cm^3mol^{-1}s^{-1}$. The best-fit model suggests a low-pressure-limit reaction rate constant of 2.96×10^8 $cm^3mol^{-1}s^{-1}$; an estimated 10% fitting error is assigned. In addition to the fitting uncertainty, uncertainty in temperature is the other major source of error. As discussed in an earlier study [21], the initial temperature immediately behind the reflected shock wave is determined from the measured incident shock speed. The combined uncertainty in temperature is estimated to be ±11 K, resulting in an associated uncertainty in the measured reaction rate constant of ±21%. Combining uncertainties in fitting and temperature, we estimate the overall uncertainty to be ±23%. A similar uncertainty level (±23%) was claimed in an earlier study using a similar methodology [21].

The measured rate constants of R1 (M = Ar) near its low-pressure limit is tabulated in Table 1 and are shown on an Arrhenius plot in Fig. 3. Troe [24] conducted a systematic experimental and review study for hydrogen peroxide decomposition and suggested a reaction rate constant for this reaction over a wide range of pressures. Most of the recently developed kinetic mechanisms use Troe's suggested rate constant [5,6,30]. However, recent studies utilizing on advanced laser diagnostics have suggested that Troe's expression slightly overpredicts the actual rate constant [21–23]. As shown in Fig. 3, our measurements corroborate the findings of these studies. Therefore, we will adopt the reaction rate constant suggested by Hong [21] for next step analysis, which is given by $k_{0,Ar}$.

$$k_{0,Ar} = 10^{15.97} e^{\frac{-21,220}{T}} \; cm^3 mol^{-1} s^{-1} \tag{4}$$

3.2. Rate constant measurement and determination of $H_2O_2+CO_2 \rightarrow 2OH+CO_2$ using Chemkin Pro

The test mixture chosen for determining the rate constant of R1(M = CO_2) had 20% CO_2/80% Ar as the bath gas. The concentration of CO_2 was limited to 20% to mitigate impact of shock bifurcation and accompanying non-uniformities in the test gas mixture. This is confirmed by a comparison of the pressure traces measured in a mixture with and without CO_2 (Fig. 4). Notably, pressure change during the test time is close to zero in both cases by using a driver insert.

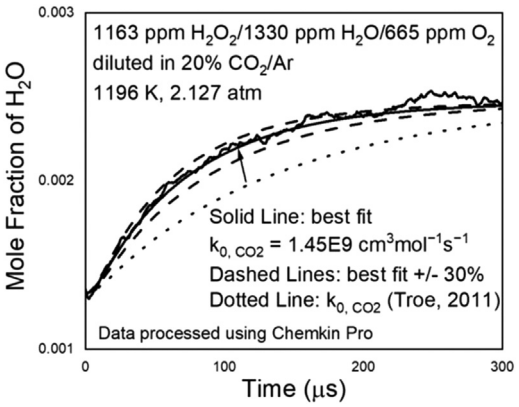

Fig. 5. Measured water time history and the best-fit rate constant ($k_{0,CO2} = 1.45 \times 10^9$ $cm^3mol^{-1}s^{-1}$, using Chemkin Pro) with a mixture of 1163 ppm H_2O_2/1330 ppm H_2O/665 ppm O_2/20% CO_2/Ar at 1196 K, 2.127 atm.

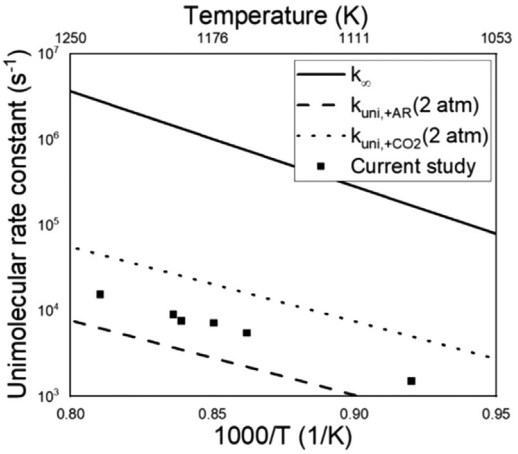

Fig. 6. Comparison between the measured H_2O_2 decomposition rate constants (data processed using Chemkin Pro) with the high-pressure-limit and low-pressure-limit rate constants. The solid line is the unimolecular high-pressure limit from Ref. [24]; the dashed line is the unimolecular reaction rate for M = Ar from Ref. [21]; the dotted line is the inferred unimolecular reaction rate for M=CO_2 from this study; the points are the unimolecular reaction rate for $M = 20\%$ CO_2/Ar determined in this study.

The water time histories are sensitive to both R1(M = Ar) and R1(M = CO_2) at the experimental conditions. Since the rate constant of R1(M = Ar) has already been determined within tight uncertainty bounds (Section 3.1), the rate constant of R1(M = CO_2) can be inferred from the measured time histories. Again, the contribution of secondary reactions to the sensitivity of water time histories is small compared to R1(M = Ar) and R1(M = CO_2).

The fitting procedure followed for determining R1 (M = CO_2) was the same as the procedure followed for R1 (M = Ar). The low-pressure limit of the rate constant of R1 (M = CO_2) was adjusted until the simulated water time histories matched the measured water time histories using Chemkin Pro. A representative water time history measured in one of these experiments is shown in Fig. 5. Also shown is the mole-fraction time history based on the unperturbed model which uses Troe's suggested chaperon efficiency for CO_2 in the single equation format describing R1. The best-fit time history is also shown on the plot, along with the time histories corresponding to the 30% uncertainty bounds. For this representative experiment, the chaperon efficiency for CO_2 had to be raised about 3.5 times to match our measurements. Similar values were obtained for experiments conducted at other temperatures, as shown in the Supplementary Material. This analysis relies on the traditional linear mixing rule and provides a collision efficiency for our mixture of 20% CO_2 in Argon. These determined values are shown in Table 2 and Fig. 6.

The initial temperature immediately behind the reflected shock wave was the major source of uncertainty, resulting in an uncertainty of ±21% in the measured rate constant. The uncertainty in the only other dominant reaction, R1(M = Ar) also contributes to the uncertainty in the rate constant of R1 (M = CO_2). The uncertainty in the rate constant of R1(M = Ar) was found to be ±23% (Section 3.1). This results in an uncertainty of ±9% in the rate constant of R1(M = CO_2). Combining uncertainties in fitting, other interfering reactions, with the aforementioned sources of uncertainty, we estimated the overall uncertainty in the rate constant of R1(M = CO_2) to be ±32%.

3.3. Rate constant determination of $H_2O_2+CO_2 \rightarrow 2OH+CO_2$ using the reduced pressure-based linear mixing rule (LMR,R)

One of the concerns in determining the rate constant of R1(M = CO_2) from mixtures containing both argon and carbon dioxide bath gasses is the validity of linear mixing rules towing to the variation in the relative effectiveness of these bath gasses in stabilization of the excited decomposition products [31–33]. To clarify, the decomposition rate of hydrogen peroxide can depart from the mole fraction weighted linear sum of reaction rate constants of R1 (M = Ar) and R1 (M = CO_2). Matsugi [34] conducted a modeling study of third-body effects in the thermal decomposition of H_2O_2 by classical trajectory calculations of the collisional energy transfer processes and master equation analyzes of the pressure-dependent rate constants. In his analysis, the reduced pressure-based linear mixture rule (LMR,R) proposed by Burke and Song [35] can closely reproduce the rate constants cal-

Table 2
Reaction rate constant measurement of $H_2O_2 + CO_2 \rightarrow 2OH + CO_2$.

T (K)	P (atm)	$[H_2O_2]$ (ppm)	$k_{0,CO2}$ ($cm^3mol^{-1}s^{-1}$)	$k_{0,CO2,R}$ ($cm^3mol^{-1}s^{-1}$)
1160	2.1	624	8.53×10^8	3.13×10^8
1192	2.1	507	1.21×10^9	4.53×10^8
1234	2	1045	2.55×10^9	9.59×10^8
1196	2.1	1163	1.45×10^9	5.38×10^8
1176	2.1	1147	1.13×10^9	4.15×10^8
1087	2.3	492	2.20×10^8	7.87×10^7

culated by the master equation. The deviations between the two are subtle and at most −2.6%. The reaction rate constant discrepancy between the reduced pressure-based linear mixture rule and the traditional linear mixture rule (LMR,P) can be derived from the two formulations. The equations for LMR, R and LMR, P are provided by Burke and Song [35]:

$$LMR,\ P:\ k_{LMR,P}(T,P,\underline{X}) = \sum\nolimits_i k_i(T,P)X_i \quad (5)$$

$$LMR,\ R:\ k_{LMR,R}(T,P,\underline{X}) = k_\infty(T)\,(R_{LMR}/(1+R_{LMR}))\left(\sum\nolimits_i F_i(T,R_{LMR})\tilde{X}_{i,LMR}\right)\right) \quad (6)$$

Where,

$$R_{LMR}(T,P,\ \underline{X}) = \sum\nolimits_i k_{0,i}(T)X_i[M]/k_\infty(T) \quad (7)$$

$$F_i(T,R_{LMR}) = k_i(T,R_{LMR})/k_\infty(T)/\left(\frac{R_{LMR}}{(1+R_{LMR})}\right) \quad (8)$$

$$\tilde{X}_{i,LMR}(T,P,\ \underline{X}) = k_{0,i}(T)X_i/\sum\nolimits_j k_{0,j}(T)X_j \quad (9)$$

The inferred rate constants using LMR,R, $k_{0,CO2,R}$, are also tabulated in Table 2. $k_{0,CO2,R}$ can be used in software packages having LMR,R or other nonlinear mixing rules.

The $k_{0,CO2}$ values are the Chemkin Pro (traditional linear mixing rule) inferred reaction rate constants (derivable when using the single equation with chaperon efficiencies, as might be used in the CHEMKIN software suite) and can only be used for the mixtures with about 20% CO_2. Fig. 7 shows the comparison of LMR,R and LMR,P for Ar/CO_2 mixtures at 2 atm and 1200 K. The ratio of the reaction rate constant, $k_{LMR,R}/k_{LMR,P}$, can be as high as 2.3. Therefore, the mixing rule used in the data reduction can lead to very different results in the inferred rate constant.

Fig. 8 shows the comparison between our measurements and the rate constants reported in literature. For the low-pressure-limit reaction rate constant of $H_2O_2+CO_2 \rightarrow 2OH+CO_2$, there are two

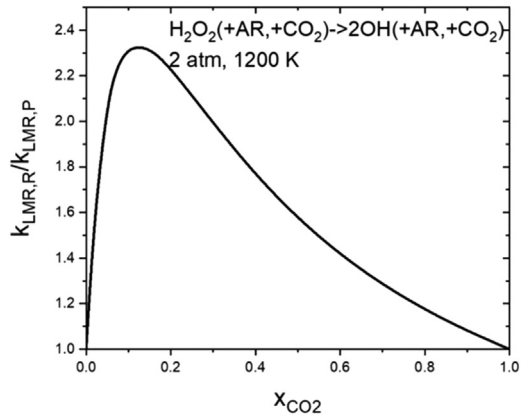

Fig. 7. Comparison of LMR,R and LMR,P for Ar/CO_2 mixtures at 2 atm and 1200 K.

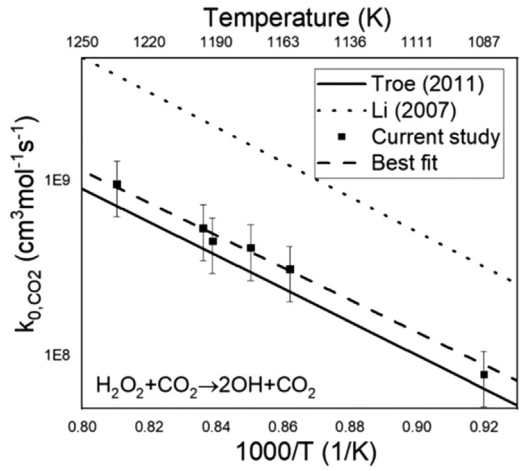

Fig. 8. Comparison of the measured reaction rate constant, $k_{0,CO2,R}$, of $H_2O_2+CO_2 \rightarrow 2OH+CO_2$ with literature studies in low-pressure-limit.

commonly used reaction rate constants found in the combustion kinetic mechanism literature. The solid line shows the reaction rate constant suggested by Troe in a review study [24] considering an experimental study conducted in 1956 [25],

which has been adopted by several recent mechanisms, including FFCM [5], ARAMCO [6], and NUI-Syngas [30]. On the other hand, the dotted line shows another reaction rate constant used by Li et al. [36,37], which has been adopted by other mechanisms, such as the LLNL n-alkane models [38,39] and the CSE mechanism [40]. The Li et al. rate constant has a value that is approximately five times the Troe rate constant. Our measurements of this rate constant are the first to be reported in the literature. As shown in Fig. 8, our measured rate constants are close to Troe's [24] rate constant. We suggest the following expression as the low-pressure-limit rate constant for R1 (M = CO_2) determined over the temperature range of 1087–1234 K.

$$k_{0,CO2,R} = 10^{16.43\pm0.12} e^{\frac{-21,220\pm250}{T}}\ cm^3 mol^{-1} s^{-1} \quad (10)$$

4. Conclusion

The rate constant of decomposition of hydrogen peroxide with argon and carbon dioxide as bath gasses, was measured in the temperature range between 1087 and 1234 K and at a pressure of 2.0–2.4 atm. The measured rate constants were near their respective low-pressure limits. The measured reaction rate constants of H_2O_2+Ar $\rightarrow 2OH+Ar$ were found to be in very good agreement with the expression proposed by Hong et al. [21]. The R1 rate constant for [M] = [CO_2] reaction is given by Eq. (10).

To the best of our knowledge, the reaction rate constant measurement of H_2O_2+CO_2 $\rightarrow$ 2OH+CO_2 is the first in the current temperature range and mixture. Our measurements suggest that the reaction rate constant is consistent with a commonly used value given by Troe [24] when allowance is made for the LMR,R mixing rule.

Further rate constant determination experiments with a range of CO_2 mole fractions that would provide validation of the LMR,R mixing rule are recommended.

Declaration of Competing Interest

The authors declare that they have no known competing financial interests or personal relationships that could have appeared to influence the work reported in this paper.

Acknowledgments

This work was supported by U.S. Department of Energy under grant number DE-SC0019634. We would like to thank the many colleagues who have reminded us about the role of the mixing rule in the analysis of these experiments.

Supplementary materials

Supplementary material associated with this article can be found, in the online version, at doi: 10.1016/j.proci.2022.08.021.

References

[1] Annual Energy Outlook 2021. Available at https://www.eia.gov/outlooks/aeo/.
[2] SCO2 power cycles. Available at https://www.energy.gov/sco2-power-cycles.
[3] A. McClung, Oxy-combustion integration for direct fireds CO2 cycles, in: Proceedings of the Fifth International Symposium-Super-Critical CO_2 Power Cycles, 2016, pp. 28–31.
[4] J. Shao, R. Choudhary, D.F. Davidson, R.K. Hanson, S. Barak, S. Vasu, Ignition delay times of methane and hydrogen highly diluted in carbon dioxide at high pressures up to 300 atm, Proc. Combust. Inst. 37 (2019) 4555–4562.
[5] G.P. Smith, Y. Tao, and H. Wang, Available at https://web.stanford.edu/group/haiwanglab/FFCM1/pages/FFCM1.html
[6] C.W. Zhou, Y. Li, U. Burke, C. Banyon, K.P. Somers, S. Ding, S. Khan, J.W. Hargis, T. Sikes, O. Mathieu, E.L. Petersen, M. AlAbbad, A. Farooq, Y. Pan, Y. Zhang, Z. Huang, J. Lopez, Z. Loparo, S. Vasu, H.J. Curran, An experimental and chemical kinetic modeling study of 1, 3-butadiene combustion: ignition delay time and laminar flame speed measurements, Combust. Flame 197 (2018) 423–438.
[7] M. Karimi, B. Ochs, Z. Liu, D. Ranjan, W. Sun, Measurement of methane autoignition delays in carbon dioxide and argon diluents at high pressure conditions, Combust. Flame 204 (2019) 304–319.
[8] M.P. Burke, M. Chaos, F.L. Dryer, Y. Ju, Negative pressure dependence of mass burning rates of H_2/CO/O_2/diluent flames at low flame temperatures, Combust. Flame 157 (2010) 618–631.
[9] H. Wang, D.A. Sheen, Combustion kinetic model uncertainty quantification, propagation and minimization, Prog. Energy Combust. Sci. 47 (2015) 1–31.
[10] F. vom Lehn, L. Cai, H. Pitsch, Sensitivity analysis, uncertainty quantification, and optimization for thermochemical properties in chemical kinetic combustion models, Proc. Combust. Inst. 37 (2019) 771–779.
[11] P.A. Strakey, Oxy-combustion modeling for direct–fired supercritical CO_2 power cycles, J. Energy Res. Technol. 141 (2019) 070706.
[12] A.E. Masunov, E.E. Wait, S.S. Vasu, Catalytic effect of carbon dioxide on reaction OH+ CO$\rightarrow$ H+ CO_2 in super-critical environment: master equation study, J. Phys. Chem. A 122 (2018) 6355–6359.
[13] E.E. Wait, A.E. Masunov, S. Vasu, Quantum chemical and master equation study of OH+ $CH_2O\rightarrow$ H_2O+ CHO reaction rates in super-critical CO_2 environment, Int. J. Chem. Kinet. 51 (2019) 42–48.
[14] J. Shao, R. Choudhary, A. Susa, D.F. Davidson, R.K. Hanson, Shock tube study of the rate constants for H+ O_2+ M$\rightarrow$ HO_2+ M (M= Ar, H_2O, CO_2, N_2) at elevated pressures, Proc. Combust. Inst. 37 (2019) 145–152.
[15] R. Choudhary, J.J. Girard, Y. Peng, J. Shao, D.F. Davidson, R.K. Hanson, Measurement of the

reaction rate of H+ O_2+ M→ HO_2+ M, for M= Ar, N_2, CO_2, at high temperature with a sensitive OH absorption diagnostic, Combust. Flame 203 (2019) 265–278.
[16] C.K. McLane, Hydrogen peroxide in the thermal hydrogen oxygen reaction I. Thermal decomposition of hydrogen peroxide, J. Chem. Phys. 17 (1949) 379–385.
[17] C.K. Westbrook, Chemical kinetics of hydrocarbon ignition in practical combustion systems, Proc. Combust. Inst. 28 (2000) 1563–1577.
[18] E. Meyer, H.A. Olschewski, J. Troe, H.G. Wagner, Investigation of N_2H_4 and H_2O_2 decomposition in low– and high-pressure shock waves, Proc. Combust. Inst. 12 (1969) 345–355.
[19] H. Kijewski, J. Troe, Study of the pyrolysis of H_2O_2 in the presence of H_2 and CO by use of UV absorption of HO_2, Int. J. Chem. Kinet. 3 (1971) 223–235.
[20] C. Kappel, K. Luther, J. Troe, Shock wave study of the unimolecular dissociation of H_2O_2 in its falloff range and of its secondary reactions, Phys. Chem. Chem. Phys. 4 (2002) 4392–4398.
[21] Z. Hong, A. Farooq, E.A. Barbour, D.F. Davidson, R.K. Hanson, Hydrogen peroxide decomposition rate: a shock tube study using tunable laser absorption of H_2O near 2.5 μm, J. Phys. Chem. A 113 (2009) 12919–12925.
[22] Z. Hong, R.D. Cook, D.F. Davidson, R.K. Hanson, A shock tube study of OH+ H_2O_2→H_2O+ HO_2 and H_2O_2+ M→ 2OH+ M using laser absorption of H_2O and OH, J. Phys. Chem. A 114 (2010) 5718–5727.
[23] M.B. Sajid, E. Es-sebbar, T. Javed, C. Fittschen, A. Farooq, Measurement of the rate of hydrogen peroxide thermal decomposition in a shock tube using quantum cascade laser absorption near 7.7 mm, Int. J. Chem. Kinet. 46 (2014) 275–284.
[24] J. Troe, The thermal dissociation/recombination reaction of hydrogen peroxide H_2O_2 (+ M) ⇔ 2OH (+ M) III.: analysis and representation of the temperature and pressure dependence over wide ranges, Combust. Flame 158 (2011) 594–601.
[25] D.E. Hoare, J.B. Protheroe, A.D. Walsh, The thermal decomposition of hydrogen peroxide vapour, Trans. Faraday Soc. 55 (1959) 548–557.
[26] S.J. Cassady, R. Choudhary, N.H. Pinkowski, J. Shao, D.F. Davidson, R.K. Hanson, The thermal decomposition of ethane, Fuel 268 (2020) 117409.
[27] J. Shao, A.M. Ferris, R. Choudhary, S.J. Cassady, D.F. Davidson, R.K. Hanson, Shock-induced ignition and pyrolysis of high-pressure methane and natural gas mixtures, Combust. Flame 221 (2020) 364–370.
[28] W. Ludwig, B. Brandt, G. Friedrichs, F. Temps, Kinetics of the reaction C_2H_5+ HO_2 by time-resolved mass spectrometry, J. Phys. Chem. A 110 (2006) 3330–3337.
[29] C.S. Goldenstein, J.B. Jeffries, R.K. Hanson, Diode laser measurements of linestrength and temperature-dependent lineshape parameters of H_2O-, CO_2-, and N_2-perturbed H_2O transitions near 2474 and 2482 nm, J. Quant. Spectrosc. Radiat. Transf. 130 (2013) 100–111.
[30] Y. Zhang, O. Mathieu, E.L. Petersen, G. Bourque, H.J. Curran, Assessing the predictions of a NOx kinetic mechanism on recent hydrogen and syngas experimental data, Combust. Flame 182 (2017) 122–141.
[31] L. Lei, M.P. Burke, Mixture rules and falloff are now major uncertainties in experimentally derived rate parameters for H+O_2(+ M) ↔ HO_2 (+ M), Combust. Flame 213 (2020) 467–474.
[32] L. Lei, M.P. Burke, Bath gas mixture effects on multichannel reactions: insights and representations for systems beyond single-channel reactions, J. Phys. Chem. A 123 (2018) 631–649.
[33] L. Lei, M.P. Burke, Dynamically evaluating mixture effects on multi-channel reactions in flames: a case study for the CH_3+ OH reaction, Proc. Combust. Inst. (2020), doi:10.1016/j.proci.2020.06.187.
[34] A. Matsugi, Modeling third-body effects in the thermal decomposition of H_2O_2, Combust. Flame 225 (2021) 444–452.
[35] M.P. Burke, R. Song, Evaluating mixture rules for multi-component pressure dependence: H+ O_2 (+ M)= HO_2 (+ M), Proc, Combust. Inst 36 (2017) 245–253.
[36] J. Li, Z. Zhao, A. Kazakov, M. Chaos, F.L. Dryer, J.J. Scire Jr, A comprehensive kinetic mechanism for CO, CH_2O, and CH_3OH combustion, Int. J. Chem. Kinet. 39 (2007) 109–136.
[37] J. Warnatz, Rate coefficients in the C/H/O system, in: Combustion Chemistry, Springer, New York, NY, 1984, pp. 197–360.
[38] S.M. Sarathy, C.K. Westbrook, M. Mehl, W.J. Pitz, C. Togbe, P. Dagaut, H. Wang, M.A. Oehlschlaeger, U. Niemann, K. Seshadri, P.S. Veloo, C. Ji, F.N. Egolfopoulos, T. Lu, Comprehensive chemical kinetic modeling of the oxidation of 2-methylalkanes from C7 to C20, Combust. Flame 158 (2011) 2338–2357.
[39] S.M. Sarathy, C. Yeung, C.K. Westbrook, W.J. Pitz, M. Mehl, M.J. Thomson, An experimental and kinetic modeling study of n-octane and 2-methylheptane in an opposed-flow diffusion flame, Combust. Flame 158 (2011) 1277–1287.
[40] P. Gokulakrishnan, S. Kwon, A.J. Hamer, M.S. Klassen, R.J. Roby, Reduced kinetic mechanism for reactive flow simulation of syngas/methane combustion at gas turbine conditions, in: Proceedings of the Turbo Expo: Power for Land, Sea, and Air, 42363, 2006, pp. 513–521.